Extracellular matrix dermatopontin modulates prostate cell growth *in vivo*

Takumi Takeuchi, Motofumi Suzuki, Jimpei Kumagai, Toshiyuki Kamijo, Masato Sakai and **Tadaichi Kitamura**

Department of Urology and Andrology, Faculty of Medicine, University of Tokyo, 7-3-1 Hongo, Bunkyo-ku, Tokyo 113-8655, Japan
(Requests for offprints should be addressed to T Takeuchi; Email: nezu-tky@umin.ac.jp)

Abstract

Dermatopontin is a tyrosine-rich acidic extracellular matrix protein of 22 kDa with possible functions in cell–matrix interactions and matrix assembly. We have previously isolated mRNAs expressed in hormone-refractory, but not in hormone-sensitive, mouse mammary cancer by comparing the mRNAs expressed in either tumor. A partial mRNA sequence isolated was later proven to be a part of mouse dermatopontin mRNA sequence. Transfectants of mouse dermatopontin cDNA into PC-3 human prostate cancer cells enhanced tumor growth when those were implanted subcutaneously in nude mice compared with the controls. Those transfectants showed a prominent stroma compared with the controls. Localization of the targets of a fusion protein of mouse dermatopontin and alkaline phosphatase was in the stroma of the PC-3 tumor tissues, but not in the tumor cells themselves. Additionally, we have established mouse dermatopontin transgenic mice under the control of the rat probasin promoter. The prostatic dorsal lobes of dermatopontin transgenic mouse showed prostate intraepithelial neoplasia at the age of 11 months, but the control littermates did not. Epithelium of other prostatic lobes was not markedly different from that of the controls. In conclusion, dermatopontin may be involved in the pathogenesis and growth of the prostate cancer.

Journal of Endocrinology (2006) **190,** 351–361

Introduction

Dermatopontin is a tyrosine-rich acidic extracellular matrix protein of 22 kDa with possible functions in cell–matrix interactions and matrix assembly (Neame *et al.* 1989, Superti-Furga *et al.* 1993, Forbes *et al.* 1994). Human dermatopontin has 96% identity to the bovine sequence and its expression is not limited to the connective tissue, as northern blots show specific mRNAs in cultured fibroblasts, the muscle, heart, pancreas, and lung (Superti-Furga *et al.* 1993). The protein was proven to associate with decorin and a modified decorin with carboxymethylated cysteinyl residues, but not to assemble to hyaluronate or dermatan sulfate chains (Okamoto *et al.* 1996).

There has been controversy as to whether dermatopontin enhances or suppresses the proliferation of cells and the accumulation of the extracellular matrices. Dermatopontin enhanced the growth-inhibitory activity of transforming growth factor (TGF)-β on mink lung epithelial cells through its interaction with decorin in the microenvironment of the extracellular matrix *in vivo* (Okamoto *et al.* 1999). Leiomyomas and keloids demonstrated reduced levels of dermatopontin (Catherino *et al.* 2004) and microarray analysis showed the downregulation of dermatopontin in leiomyoma compared with myometrium (Tsibris *et al.* 2002). The decreased expression of dermatopontin is associated with the pathogenesis of fibrosis in hypertrophic scar and systemic sclerosis (Kuroda *et al.* 1999). Additionally, stably transfected BALB/c 3T3 cells expressing mouse dermatopontin showed approximately 50% inhibition of cell proliferation (Tzen & Huang 2004).

Conversely, dermatopontin knockout mice did not exhibit any obvious anatomical abnormality, but showed a significant decrease in the relative thickness of the dermis compared with wild-type mice and 40% lower skin collagen content, indicating that dermatopontin plays a critical role in the elasticity of skin and collagen accumulation attributed to collagen fibrillogenesis *in vivo* (Takeda *et al.* 2002). The infarct zone of experimentally induced myocardial infarction in rats showed the increased expression of dermatopontin mRNA in macrophages and spindle-shaped mesenchymal cells (Takemoto *et al.* 2002).

We have previously isolated mRNAs expressed in hormone-refractory but not in hormone-sensitive mouse mammary cancer (Shionogi carcinoma) by comparing mRNAs expressed in both kinds of tumor (Takeuchi *et al.* 2000) using a suppressive subtractive hybridization method (Diatchenko *et al.* 1996). A partial mRNA sequence isolated there was later proven to be a part of mouse dermatopontin mRNA sequence, which has 92%

DOI: 10.1677/joe.1.06619
0022–0795/06/0190–351
Online version via http://www.endocrinology-journals.org

homology to human dermatopontin (Tzen & Huang 2004). Thus, we tested the functions of dermatopontin in cancer growth *in vivo* with a xenogenic tumor graft model. In other words, we have established mouse dermatopontin transfectants of PC-3 human prostate cancer cells and subcutaneously implanted them into the flanks of nude mice to assess tumor growth. Additionally, we have established mouse dermatopontin transgenic mice under the control of rat probasin (prostate basic protein) promoter and analyzed prostatic histology. Probasin is an androgen-dependent and prostate-specific secretory protein produced in differentiated prostatic epithelial cells. Short rat probasin promoter (−426 to +34) is used to establish transgenic mice expressing genes in the prostatic epithelial cells (Rennie *et al.* 1993).

Materials and Methods

Constructs of vectors

pCGAAS-mEQ1 Mouse cDNA encoding full-length mouse dermatopontin was excised with XbaI and HindIII from pEQ1 (pUC18 containing mouse dermatopontin) provided from Dr C Y Tzen (Mackay Memorial Hospital, Taipei, Taiwan), blunted with Klenow fragment, gel purified and ligated into the EcoRI site of the mammalian expression vector pCAGGS (Niwa *et al.* 1991) blunted with a Klenow fragment in a sense direction, yielding pCGAAS-mEQ1. pCAGGS was provided by Dr J Miyazaki (Osaka University, Osaka, Japan).

pBH-mEQ1polyA pBH500 vector containing the 5′-flanking region of the rat probasin gene provided by Dr R J Matusik (Vanderbilt University, Nashville, TN, USA) was digested with HindIII, blunted with Klenow DNA polymerase, digested with BamHI, then electrophoresed. The 454 bp fragment of pBH500, including the rat probasin promotor region, was gel purified and ligated between the KpnI site blunted with the Klenow and cohesive BamI site of the pUC18 vector, resulting in the pUC18-probasin vector. The XbaI-HindIII fragment of pCGAAS-mEQ1, containing mouse dermatopontin cDNA and the rabbit β-globin polyA signal, was ligated between the XbaI and HindIII sites of pUC18-probasin, yielding the pBH-mEQ1polyA vector, which expresses mouse dermatopontin under the control of rat probasin promotor.

pAPTag5-mEQ1 pAPTag5 vector (GenHunter Corporation, Nashville, TN, USA) was digested with Hind III and Bgl II and blunted with Klenow DNA polymerase. pEQ1, pUC18 containing mEQ1, was digested with XbaI, blunted with a Klenow fragment, digested with HindIII, then electrophoresed. The Hinc II fragment of mouse dermatopontin cDNA described above was ligated into the pAPTag5 described above yielding pAPTag5-mEQ1. Thus, pAPTag5-mEQ1 produces a fusion protein of mouse dermatopontin and alkaline phosphatase (f-DPN-AP) without frame shift. All vector constructs were confirmed by sequencing. pAPTag5 vector was used as the control vector.

Stable mouse dermatopontin transfectants of PC-3 human prostate cancer cells

pCGAAS-mEQ1 and control pCGAAS vectors were co-transfected together with neomysin-resistant gene (Takeuchi *et al.* 1996) by a molar ratio of 5:1 into PC-3 human prostate cancer cells using lipofectamine (Gibco BRL) following the manufacturer's instructions. Stable transfectants were cloned in RPMI1640 medium containing 10% fetal calf serum and 400 μg/ml of G418. Genomic DNA and total RNA were extracted as previously described (Takeuchi *et al.* 1999). Genomic integration of transfected genes were tested by PCR of genomic DNA using a sense primer taken from the 5′-upstream vector sequence (5′-GCAACGTGCTGGTTGTTGTG-3′)/an antisense primer (5′-GTCAGAGCCTTCCTTCTTGC-3′) taken from a sequence of mouse dermatopontin cDNA and/or a sense primer (5′-GGTGGCTACGGGTACCCATA-3′) taken from a sequence of mouse dermatopontin cDNA/an antisense primer (5′-ACCTCCTTCTGATAGGCAG-3′) taken from a 3′-downstream vector sequence amplifying junctional DNA sequences followed by electrophoresis in 2% agarose gel. Control pCGAAS transfectants were tested by the PCR of genomic DNA using primers of 5′-upstream and 3′-downstream vector sequences flanking the EcoRI cloning site. Reverse transcriptase (RT)-PCR of mouse dermatopontin and human glyceraldehydes-3-phosphate dehydrogenase (GAPDH) mRNAs was performed from 2 μg total RNA essentially as previously described (Takeuchi *et al.* 1999) using sense/antisense primers 5′-GGTGGCTACGGGTACCCATA-3′/5′-GTCAGAGC-CTTCCTTCTTGC-3′ and those for human GAPDH (SP-10231) purchased from Maxim Biotech, Inc. (South San Francisco, CA, USA) respectively. Human dermatopontin mRNA was amplified as above by PCR using the sense/antisense primers 5′-CCTGGGGCCAGTATGGCGAT-3′/5′-ATGCTCCTCACGGCCACTAT-3′.

Anti-mouse dermatopontin polyclonal antibody

Anti-mouse dermatopontin polyclonal antibodies were produced by immunizing rabbits following a Eurogentec program (The Double XP System for peptide immunization, http://www.eurogentec.de) with a mixture of two kinds of peptides (FIMCRMTDYDCEFENV-COOH and aa 62–77: IFSKKEGSDRQWNYAC) designed from mouse dermatopontin protein. Additionally, antisera were purified by affinity against each of the peptides used for antibody production. This allows to obtain specific antibodies against each of the peptides separately.

Fusion protein of mouse dermatopontin and alkaline phosphatase

pAPTag5-mEQ1 vector and pAPTag5 vector were transfected into 293T cells using DoFect GT1 (Dojindo Laboratories,

Kumamoto, Japan) following the manufacturer's instructions. Stable transfectants were cloned in Dulbecco's Modified Eagle's Medium (DMEM) containing 10% fetal calf serum and 200 μg/ml of zeocin. The genomic integration of pAPTag5-mEQ1 and pAPTag5 was confirmed by PCR of the junctional region using a sense primer (5′-GGTGGCTACGGGTACC-CATA-3′) taken from the sequence of mouse dermatopontin cDNA/R-AP primer (GenHunter Corporation) taken from the 3′-downstream pAPTag5 vector sequence for the former, and L-AP primer (GenHunter Corporation) taken from the 5′-uptream pAPTag5 vector sequence/R-AP primer for the latter. Expression of f-DPN-AP was assessed by Western analysis using anti-mouse dermatopontin polyclonal antibody as below. Culture supernatants of those clones were stored at −80 °C until use.

Western analysis

Cells and tissue specimens were lysed in Nonidet P-40 lysis buffer (50 mM Tris–HCl (pH 7·4), 150 mM NaCl, 10 mM NaF, 5 mM EDTA, 5 mM EGTA, 2 mM sodium vanadate, 0·5% sodium deoxycholate, 1 mM dithiothreitol (DTT), 1 mM phenylmethylsulfonylfluoride (PMSF), 2 μg/ml aprotinin and 0·1% Nonidet P-40) and the lysates were centrifuged at 15 000 ***g*** for 30 min at 4 °C. Aliquots of protein (20 μg) were fractionated on SDS-12·5% polyacrylamide gels and electrophoretically transferred onto polyvinylidene difluoride (PVDF) membranes (Immobilon, Millipore Co., Bedford, MA, USA). The membranes were blocked in Tris-buffered saline (TBS) with 5% skim milk overnight, then hybridized with 1:500 diluted anti-mouse dermatopontin polyclonal antibody purified against a peptide (IFSKKEGSDRQWNYAC) at room temperature for 3 h. Each membrane was washed in TBS with 0·1% Tween 20 and incubated with 1:10 000 diluted horseradish peroxidase-conjugated donkey anti-rabbit immunoglobulin (Ig)G (Amersham Pharmacia Biotech) at room temperature for 1 h. Bands were visualized with the chemiluminescence-based ECL plus detection system (Amersham Pharmacia Biotech). The membranes were exposed to X-ray film.

MTT [3-(4,5-dimethylthiazol-2-yl)-2,5-diphenyltetrazolium-bromide] assay

Of mouse dermatopontin cDNA transfectants of PC-3 cells as well as control clones transfected with pCGAAS control vector were cultured in quadriplicate in RPMI1640 medium containing 10% fetal calf serum up to 5 days. MTT assays were performed as previously described (Takeuchi *et al.* 1996).

Xenogenic tumor model

Aliquots of 1×10^6 of mouse dermatopontin cDNA transfectants of PC-3 cells as well as control clones transfected with pCGAAS control vector suspended in 200 μl of RPMI1640 medium were implanted subcutaneously in the right flank region of male Balb/c nude mice at 5–7 weeks of age. Experiments were repeated twice.

Mouse dermatopontin transgenic mice

Transgenic mouse lines were generated by the microinjection of fertilized eggs as described previously (Takeuchi *et al.* 1999). The purified inserts of the SacI-HindIII fragment of pBH-mEQ1polyA were injected into the male pronucleus of fertilized eggs from C57BL/6L (Japan SLC, Inc., Hamamatsu, Japan) strain mice. Mice were screened for the genomic integration of the murine dermatopontin transgene as described below. Tail genomic DNA was amplified by PCR as described previously (Takeuchi *et al.* 1999) using sense/antisense primers (5′-CAGGCATTGGGCATTGTCCA-3′/5′-GTCAGAGCCTTCCTTCTTGC-3′) taken from the rat probasin promotor region upstream of the inserted cDNA and murine dermatopontin cDNA respectively. Amplified products (10 μl) were resolved by electrophoresis in 1·5% agarose gels containing ethidium bromide. Transgene-positive founder mice (F0), in addition to their littermates, were crossbred with naive C57BL/6L and naive C3H/HeN (Nihon Clea, Tokyo, Japan) mice. The studies were approved by the authors' institutional committee on animal care.

Histology

Ventral, dorsolateral, and anterior lobes of the mouse prostate were separated when the mice were killed. Paraffin-embedded sections were stained with hematoxylin–eosin staining and Masson-trichrome staining.

Immunohistochemistry Cryosections (10 μm: for fibroblast growth factor (FGF)-2 and TGF-β1) fixed in 4% paraformaldehyde and paraffin-embedded sections (for dermatopontin, collagen 1, and vascular endothelial growth factor (VEGF) were blocked with 5% sheep normal serum and hybridized at room temperature for 30 min with 1:100 diluted primary antibodies (anti-human FGF-2 rabbit polyclonal antibody (S.C.-79, Santa Cruz Biotechnology Inc., Santa Cruz, CA, USA), anti-TGF-β1 rabbit polyclonal antibody (S.C.-146, Santa Cruz Biotechnology Inc.), anti-rat collagen 1 rabbit polyclonal antibody (LSL LB-1102, Gentaur Molecular Products, Brussels, Belgium), or anti-human VEGF monoclonal antibody (RDI-VEGFabm-12, Fitzgerald Industries International Inc., Concord, MA, USA)) and 1:1000 (w/v) diluted anti-mouse dermatopontin rabbit polyclonal antibody described in Western analysis. Sections were washed three times with PBS, hybridized at room temperature for 30 min with 1:100 diluted secondary antibody (biotinylated anti-rabbit donkey immunoglobulin, GE Healthcare Bio-Sciences, Uppsala, Sweden). Labeling was visualized by the avidin–biotin complex method.

Detection of targets of dermatopontin Cells grown on cover slips and cryosections (10 μm) were fixed in methanol at −80 °C for 10 min, washed three times with PBS, blocked in DMEM with 10% FCS for 10 min, and hybridized at 4 °C overnight with f-DPN-AP in DMEM with 10% FCS. After washing with PBS three times, sections were fixed in 4% paraformaldehyde, washed in PBS three times, and heated at 65 °C for 50 min in PBS to inactivate heat-sensitive endogenous alkaline phosphatase. Positive signals were visualized using AP Assay Reagent S (GenHunter Corporation) at 4 °C overnight. Specimens were counter-stained with methyl green and mounted with Crystal/Mount (Biomeda, Foster City, CA, USA).

Validation of anti-mouse dermatopontin polyclonal antibody

To assess the validity of anti-mouse dermatopontin polyclonal antibody, the concentration of SDS-polyacrilamide gel was increased from 12·5 to 15% in the western analysis. Additionally, a peptide (IFSKKEGSDRQWNYAC), which was used to immunize rabbits and purify the antibody by affinity, was mixed with anti-dermatopontin antibody for 30 min at 37 °C at a concentration of 5 or 1 μg/μl to adsorb the antibody before western analysis or immunohistochemistry respectively. Detection without primary antibody was also included in the western analysis and immunohistochemistry of dermatopontin.

Statistical analysis

The Student's *t*-test was applied to compare the MTT assay. The Mann–Whitney *U*-test was applied to compare the tumor volume. The χ^2-test was applied to compare the rate of macroscopic tumor formation.

Results

Establishment of mouse dermatopontin transfected human prostate cancer cells

PC-3 human prostate cancer cells stably transfected with a mouse dermatopontin expression vector (pCGAAS-mEQ1) were cloned. Integration of sense mouse dermatopontin cDNA into genomic DNA was assessed by PCR (data not shown). Stable PC-3 human prostate cancer cell transfectants of pCGAAS-mEQ1 vector expressed 22 kDa protein with western analysis using anti-mouse dermatopontin polyclonal antibody, while the control cells did not, as shown in Fig. 1a. Thus, this 22 kDa protein expressed by the transfection of pCGAAS-mEQ1 vector is supposed to be the mouse dermatopontin protein. Those transfectants also expressed mouse dermatopontin mRNA, while the control clones did not, as shown in Fig. 1b. Endogenous human dermatopontin mRNA was very marginally expressed by RT-PCR in mouse dermatopontin transfected PC-3 cells and control PC-3 cells transfected with the vector alone (data not shown). Additionally, targets of dermatopontin, a possible dermatopontin receptor, assessed with immunocytochemistry using f-DPN-AP, was not detected in any mouse dermatopontin transfectants of PC-3 human prostate cancer clones as well as the control clones transfected with the control vector (data not shown).

Growth of mouse dermatopontin transfected human prostate cancer cells in vitro

As shown in Fig. 1c, the growth of mouse dermatopontin-transfected PC-3 clones *in vitro* assessed by MTT assay was not more than that of control clones transfected with the control vector.

Growth of mouse dermatopontin transfected human prostate cancer cells in vivo

As shown in Fig. 1d, the growth of mouse dermatopontin-transfected PC-3 clones expressing mouse dermatopontin protein was enhanced when implanted subcutaneously in Balb/c nude mice compared with that of the control clones. In Table 1, individual tumor volume and the rate of macroscopic tumor formation at 10 weeks following inoculation of tumor cells are shown. Dermatopontin-transfected PC-3 tumors showed prominent stroma compared with control PC-3 tumors (Fig. 2a). With Masson-trichrome staining, collagen fibers were remarkable in the intratumoral stroma of dermatopontin-transfected PC-3 tumors (DPNTf1), while the control PC-3 tumors showed mainly peritumoral collagen fibers (Fig. 2a). Cellular component of the stroma seems mainly fibroblasts in the histology. In one of eight mice bearing DPNTf1, liver metastasis was identified (Fig. 2c), but not in mice with control PC-3 tumors (statistically not significant according to the χ^2-test). Dermatopontin was detected with immunohistochemistry in mouse dermatopontin-transfected PC-3 tumor cells, but not in the control PC-3 tumor cells. Dermatopontin was marginally detected in the interstitium, regardless of dermatopontin transfection. Collagen 1 was detected in the stroma and tumor cells both in mouse DPNTf1 and in the control PC-3 tumors (Fig. 2a). VEGF was slightly detected in the stroma of DPNTf1 (Fig. 2a). FGF-2 and TGF-β1 were detected in PC-3 tumor cells regardless of dermatopontin transfection. They were also detected in the stromal cells of PC-3 tumors, especially in the DPNTf1 (Fig. 2d). Targets of dermatopontin assessed with immunohistochemistry using f-DPN-AP were detected in the stroma of the mouse dermatopontin transfected PC-3 tumor tissues, as well as the control PC-3 tumor tissues, but not in the tumor cells themselves (Fig. 2a). PC-3 tumor tissues hybridized with control AP (supernatant of pAPTag5-transfected 293 cells) did not show positive signals (data not shown).

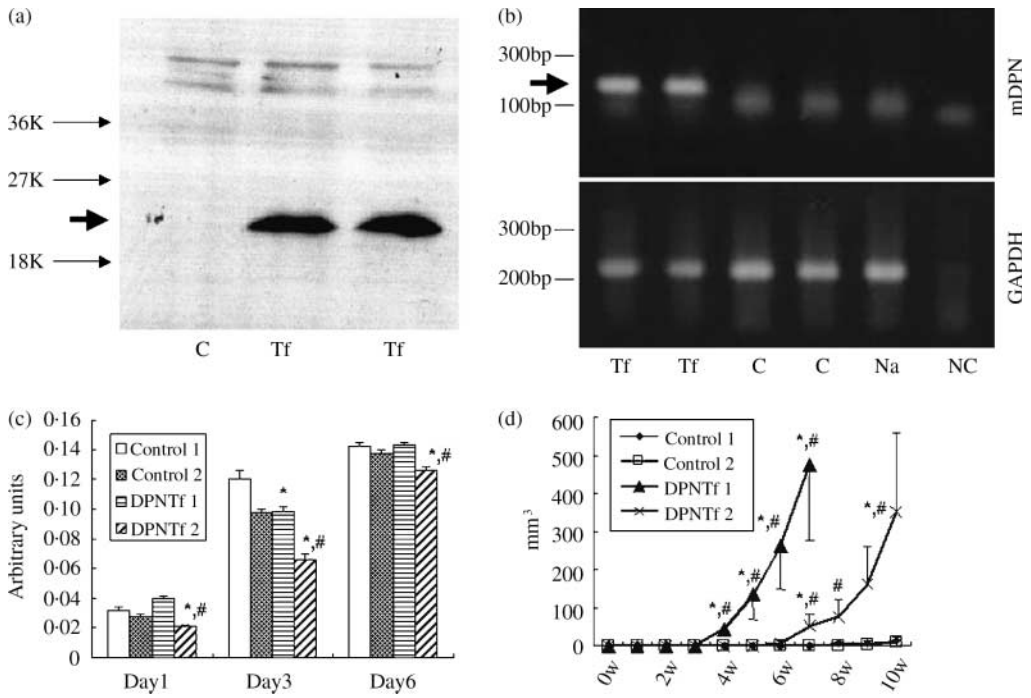

Figure 1 (a) Western blot analysis of dermatopontin protein (indicated by the arrow) by mouse dermatopontin-transfected PC-3 clones; C, control PC-3 cells; Tf, mouse dermatopontin-transfected PC-3 cells. (b) RT-PCR analysis of mouse dermatopontin mRNA (indicated by the arrow) by mouse dermatopontin-transfected PC-3 clones; C, contro PC-3 cells; Tf, mouse dermatopontin-transfected PC-3 cells; Na, naive PC-3; NC, negative control (no cDNA added). (c) Growth of mouse dermatopontin-transfected PC-3 clones in vitro by MTT assay; controls 1 and 2, PC-3 clones transfected with a vector alone; DPNTf 1 and -2, mouse dermatopontin-transfected PC-3 clones; bar, standard error; *, $P<0{\cdot}05$ vs control 1; #, $P<0{\cdot}05$ vs control 2 by the Student's *t*-test. (d) Growth of mouse dermatopontin-transfected PC-3 clones in a xenograft tumor model; controls 1 and 2, PC-3 clones transfected with a vector alone; DPNTf1 and 2, mouse dermatopontin-transfected PC-3 clones; bar, standard error; $n=12$ and 14 for controls 1 and -2 respectively; $n=14$ and 12 for DPNTf1 and -2 respectively; *, $P<0{\cdot}05$ vs control 1; #, $P<0{\cdot}05$ vs control 2; Mann–Whitney *U*-test.

Fusion protein of mouse dermatopontin and alkaline phosphatase

The genomic integration of pAPTag5-mEQ1 into 293T cell clones was confirmed by PCR of the junctional region (data not shown) and the expression of f-DPN-AP in those clones was shown at 95 kDa as Fig. 2b by Western analysis.

Establishment of mouse dermatopontin transgenic mice

Among 46 newborn C57BL/6 mice, five (two males and three females) were positive for the mouse dermatopontin transgene (Fig. 3a). The whole prostates of mouse dermatopontin transgenic mice (F_1 [C57BL/6L×C3H/HeN]) and control littermates were used for western analyses. At the age of 6 months, the transgenic lines 2 and 8 established from female founder mice upregulated dermatopontin protein in the prostate, but the control littermate did not (Fig. 3b), then proceeded to histological analysis. All other transgenic lines did not upregulate the dermatopontin protein in the prostate compared with their control littermates. Transgene transmission rates when transgenic F0 was crossed with normal C3H/HeN mice were 22 and 36% for lines 2 and 8 respectively.

Targets of mouse dermatopontin assessed by f-DPN-AP was not detected in the prostatic glandular epithelium of the ventral, dorsal, lateral, or anterior lobes of transgenic and control F_1 mice [C57BL/6L×C3H/HeN], but detected in the stroma of the prostate lobes of those mice, as shown in Fig. 3c (data of the dorsolateral lobes are representatively shown). Positive staining was also detected in abundance in the intraluminal fluid of the seminal vesicle (data not shown). Prostatic tissues hybridized with control AP did not show positive signals (data not shown).

As shown in Fig. 4a, b, and e, prostatic dorsal lobes of dermatopontin transgenic mouse lines 2 and 8 showed prostate intraepithelial neoplasia (PIN) at the age of 11 months ($n=3$ for each line), but control littermates did not. PIN was diagnosed based on the finding that there is the neoplastic proliferation of epithelial cells with nuclear atypia within preexisting or normal basement membrane confined gland spaces (Shappell *et al.* 2004). Nuclear atypia can be in the form of nuclear enlargement, nuclear membrane irregularity, hyperchromasia, chromatin clumping, prominent nucleoli, or a combination of these features.

Table 1 Growth of mouse dermatopontin-expressing PC-3 tumors

	Individual tumor volume at 10 weeks	**Rate of macroscopic tumor** (%)
Control 1	0, 0, 0, 0, 0, 0, 0, 0, 3, 14, 146	25
Control 2	0, 0, 0, 0, 0, 0, 0, 0, 0, 0, 0, 0, 128	7
DPNTf1	0, 0, 0, 0, 0, 0, >307, >804, >860, >969, >1110, >1251, >1758, >2787	57*
DPNTf2	0, 0, 0, 0, 0, 41, 60, 155, 180, 474, 820, 2480	58*

*, $P<0{\cdot}05$ vs control 2 by the χ^2-test. Tumor volumes of DPNTf1 are expressed as those at <8 weeks, because some mice were killed after 8 weeks.

The epithelium of the prostatic ventral, lateral, and anterior lobes was not markedly different from that of the controls. The stroma of all prostatic lobes of dermatopontin transgenic mice was similar to that of the control mice by hematoxylin–eosin staining. As shown in Fig. 4c, dermatopontin was detected by immunohistochemistry in the epithelium of the dorsal and ventral lobes of dermatopontin transgenic mice, but not in that of the anterior and lateral lobes of transgenic mice and that of all prostatic lobes of the control mice. The interstitium of all prostatic lobes of dermatopontin transgenic mice as well as that of the control mice, expressed dermatopontin to an extent. With Masson-trichrome staining, collagen fibers were more prominent in the stroma of the dorsal prostatic lobe of mouse dermatopontin transgenic mice than in that of the controls (Fig. 4d), but not in other prostatic lobes (data not shown). At the age of 1 month, any prostatic lobes of the mouse dermatopontin transgenic mice of both lines (2 and 8) did not show morphological differences compared with the control littermates ($n=2$ for each line, data not shown).

Validation of anti-mouse dermatopontin polyclonal antibody

Though multiple nonspecific bands were detected in the Western analysis of the mouse prostate with 12·5% gel, they have mostly disappeared by using 15% SDS-polyacrilamide gel as shown in Fig. 5a. Positive transgenic signals of dermatopontin in the western analysis of the mouse prostate (Fig. 5a) and immunohistochemistry of the epithelium of the prostatic dorsal lobe (Fig. 5b) in the transgenic mice (lines 2 and 8) were much reduced with the adsorption of the anti-dermatopontin polyclonal antibody by an antigenic peptide. Western analysis (data not shown) and immunohistochemistry (Fig. 5b) without anti-dermatopontin primary antibody showed complete negative staining.

Discussion

Transfectants of mouse dermatopontin cDNA into PC-3 human prostate cancer cells showed enhanced dermatopontin protein expression compared with control PC-3 cells, leading to enhanced tumor growth when mouse dermatopontin-transfected tumor cells were implanted subcutaneously in nude mice compared with the controls. Endogenous human dermatopontin mRNA was marginally expressed by RT-PCR both in mouse dermatopontin transfectants and control PC-3 cells, but this did not lead to dermatopontin protein detection by Western analysis. This may be because of the very low expression of endogenous human dermatopontin in PC-3 cells. There are two possibilities why dermatopontin has enhanced the PC-3 tumor growth *in vivo*. Dermatopontin itself is an extracellular matrix, thus increases the stroma, including collagen 1. The increased stroma may have the possibility to support the tumor growth by supplying blood and nutrition. This is based on the fact that dermatopontin-expressing PC-3 tumors showed more prominent intratumoral stroma than control tumors. Actually, there is VEGF expression in the stroma of dermatopontin-expressing PC-3 tumors, but this may just indicate that they have more stroma.

Another possibility is that dermatopontin is functioning as a growth factor. As the growth of mouse dermatopontin-transfected PC-3 cells *in vitro* was only slightly different from that of the control cells, a paracrine mechanism rather than an autocrine one, such as the enhanced production of growth factors by stromal cells in the tumor microenvironment, may be involved in this enhancement of PC-3 tumor growth directly or indirectly. In other words, the dermatopontin produced by tumor cells may be upregulating the production of growth factors by stromal cells. Receptor(s) of dermatopontin are yet to be identified; thus, we engineered a f-DPN-AP and utilized it instead of an anti-dermatopontin receptor antibody by hybridizing it against the targets of dermatopontin. PC-3 tumor cells did not express the targets of dermatopontin either *in vitro* or *in vivo*, regardless of the engineered expression of mouse dermatopontin in PC-3 cells. However, stromal cells in mouse dermatopontin-expressing PC-3 tumors and those in control tumors expressed the targets of dermatopontin *in vivo*. Though the similarity between mouse and human dermatopontin cDNAs is sufficiently enough (92%), of course, there is the possibility that the mouse dermatopontin in part of the fusion protein may not detect the targets of human dermatopontin, which should be expressed in PC-3 human prostate cancer cells if it exists on them. There is the possibility that the fusion protein may combine with other extracellular matrices other than the dermatopontin receptor. The positive signal detected in the intraluminal fluid of the seminal vesicle of mice may indicate this.

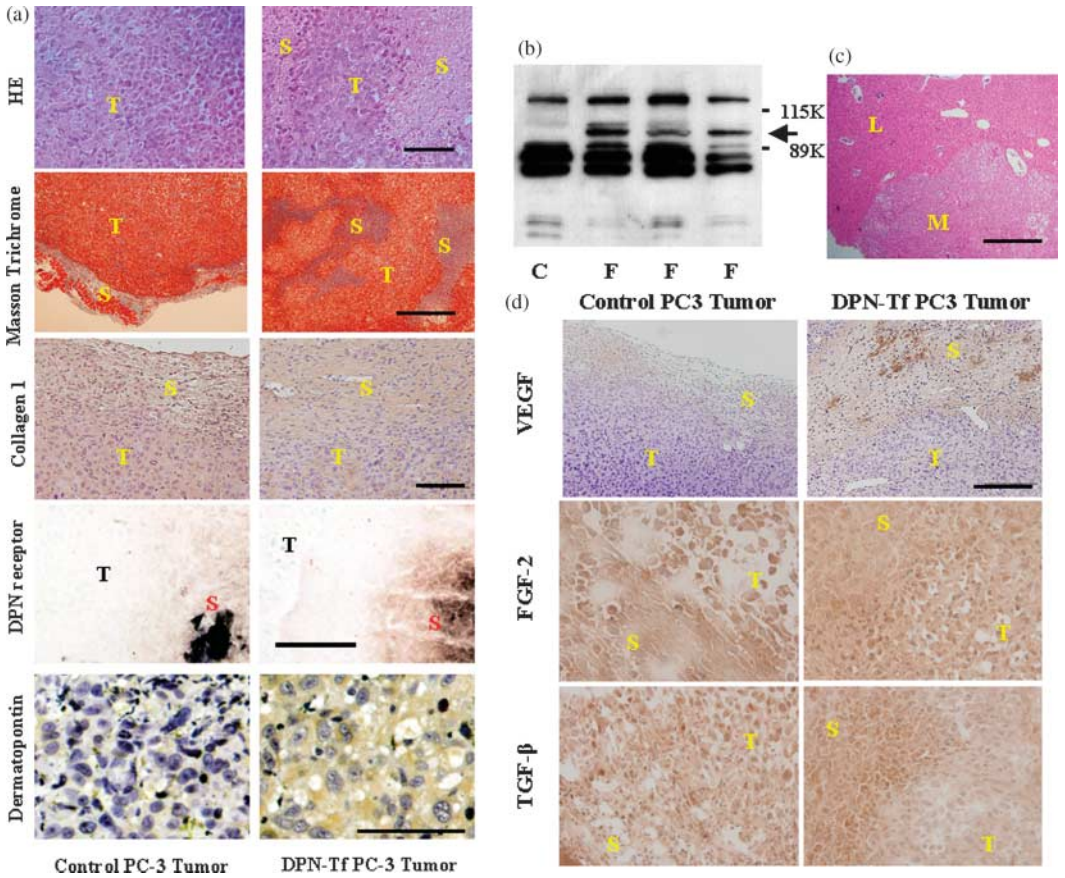

Figure 2 (a) Histology of mouse dermatopontin-transfected PC-3 tumor; T, tumor; S, stroma; top, hematoxylin–eosin staining; bar=100 μm; second, Masson-trichrome staining, bar=500 μm; third, immunohistochemistry of collagen 1, bar=100 μm; fourth, detection of dermatopontin receptor, bar=100 μm; bottom, immunohistochemistry of dermatopontin, bar=100 μm. (b) Western blot analysis of f-DPN-ALP protein by 293T cells (indicated by the arrow); C, 293T cells transfected with the pAPTag5 control vector; F, 293T cells transfected with the pAPTag5-mEQ1 vector. (c) Hepatic metastasis of mouse dermatopontin-transfected PC-3 tumor; L, normal liver; M, liver metastasis; bar=500 μm. (d) Immunohistochemistry of VEGF, FGF-2, and TGF-β1 in mouse dermatopontin-transfected PC-3 tumors; DPN-Tf, mouse dermatopontin-transfected; T, tumor; S, stroma; bar=100 μm.

As control and naive PC-3 cells do not essentially express dermatopontin protein and targets of dermatopontin (a possible dermatopontin receptor) may form an autocrine/paracrine loop within stromal cells in control and naive PC-3 tumors. In other words, dermatopontin secreted by stromal cells such as fibroblasts and endothelial cells binds to targets of dermatopontin on stromal cells and stimulates/modulates them. Then, factors released by stromal cells may stimulate/modulate tumor cells directly by paracrine mechanisms or indirectly mediated by other cells/factors. The more prominent stroma observed in dermatopontin-expressing PC-3 tumors than the controls may be evidence that dermatopontin stimulates stromal cells to proliferate and activate, and then growth factors produced by stromal cells stimulate the tumor cells leading to the formation of the tumor–stromal interactions.

In the prominent intersititum of mouse dermatopontin-expressing PC-3 tumors, TGF-β1 and FGF-2 were also expressed as well as in the PC-3 tumor cells. PC-3 cells have been reported to produce measurable amounts of FGF-2 but did not demonstrate a growth response to exogenous FGF-2, even though large amounts of FGF receptor mRNA were expressed in PC-3 cells (Nakamoto *et al.* 1992). However, FGF-2 stimulated endothelial cell proliferation *in vitro* (Hepburn *et al.* 1997) and FGF-2 maintains the survival of androgen receptor positive PC-3 clones through the positive modulation of the Bcl-2 protein and downmodulates androgen receptor (AR) protein expression, allowing the escape of selected clones from androgen regulation and the progression of prostate cancer (Rosini *et al.* 2002).

TGF-β1 and TGF-β type-1 receptor were expressed in PC-3 cells and TGF-β initially suppressed PC-3 cell growth

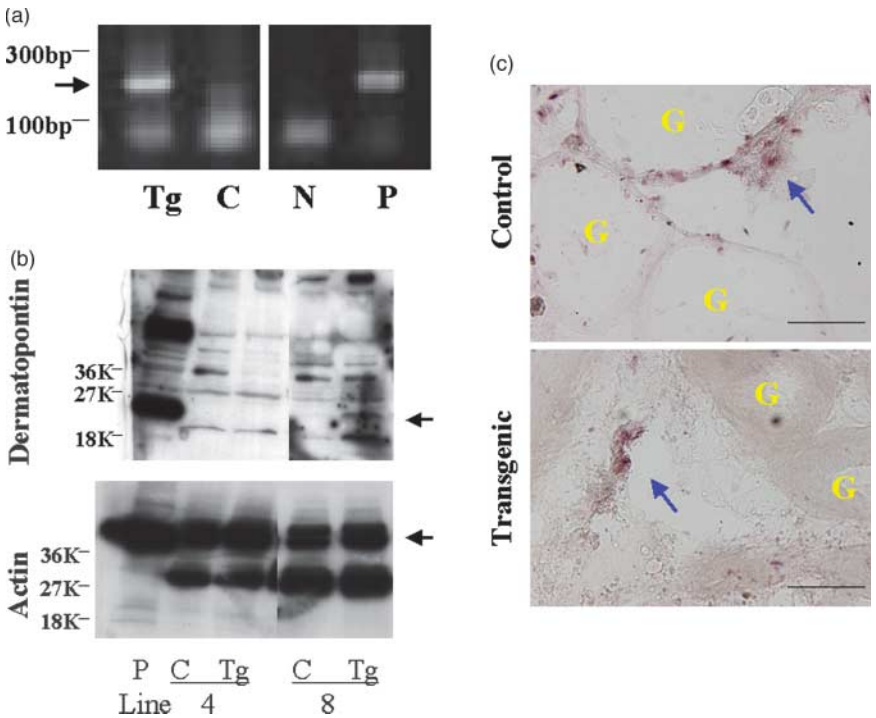

Figure 3 (a) PCR analysis of genomic integration of the murine dermatopontin transgene (indicated by the arrow); Tg, transgenic mice; C, control littermates; N, negative control (no DNA); P, positive control (pBH-mEQ1polyA vector); (b) Western blot analysis of dermatopontin protein (indicated by the arrow) and actin protein (indicated by the arrow) in the prostate of mouse dermatopontin transgenic mice at the age of 6 months; C, control littermates; Tg, transgenic mice; P, positive control (PC-3 tumor cells transfected with pCGAAS-mEQ1vector); line: transgenic lines. Line 8 is a representative of a transgenic line which expresses transgenic dermatopontin protein. Line 4 is a representative of a transgenic line which does not express transgenic dermatopontin protein. (c) Dermatopontin receptor expression in the prostatic dorsolateral lobe of mouse dermatopontin transgenic mice, bar=200 μm; G, gland; arrows, positive staining.

in vitro in a dose-dependent manner serving as an autocrine inhibitory factor in prostate cancer (Wilding *et al.* 1989, Kim *et al.* 1996). Nevertheless, TGF-β1 can influence the cellular recognition of extracellular matrix components by prostatic cancer cells and can modulate cell adhesion and invasion leading to increased invasive potential (Festuccia *et al.* 2000). Additionally, TGF-β1 enhances PC-3 matrigel invasion by an uPA/plasmin-dependent mechanism (Festuccia *et al.* 2000). Thus, as TGF-β affects a wide range of cell types, TGF-β production by prostate cancer cells may contribute an important paracrine function in the development of tumor stromal tissue and metastases, although TGF-β may directly inhibit PC-3 cell growth *in vitro*. In addition to the growth potential, forced dermatopontin expression may enhance tumor metastatic activity, because liver metastasis was observed in a host implanted with mouse dermatopontin-transfected PC-3 cells, while control mice did not show any metastasis at all in the experiment, but this was not significantly demonstrated in the experiments.

Fibrosis and keloids are associated with a decrease in the expression of dermatopontin and not an increase (Kuroda *et al.* 1999, Catherino *et al.* 2004). The discrepancy with the present data which indicate that overexpression of dermatopontin by tumor cells increased intratumoral stroma is unexplainable right now. There could be a difference in the regulation of stromal and fibrotic formation by dermatopontin between malignant and nonmalignant tissues.

We have previously established insulin-like growth factor-I (IGF-I) (Konno-Takahashi *et al.* 2003) and FGF-2 (Konno-Takahashi *et al.* 2004) transgenic mice under the control of rat probasin promoter and analyzed individual prostatic lobes of those mice, showing that both had prostatic glandular enlargement and the latter had prostatic epithelial hyperplasia like PIN in the dorsal lobe. Thus, it seems appropriate to use these types of transgenic mice to delineate effects of a given molecule on prostatic growth. In control mice, dermatopontin was not expressed in the prostatic epithelium, while the interstitium showed its expression to an extent. Nonspecific bands detected in the western analysis of the

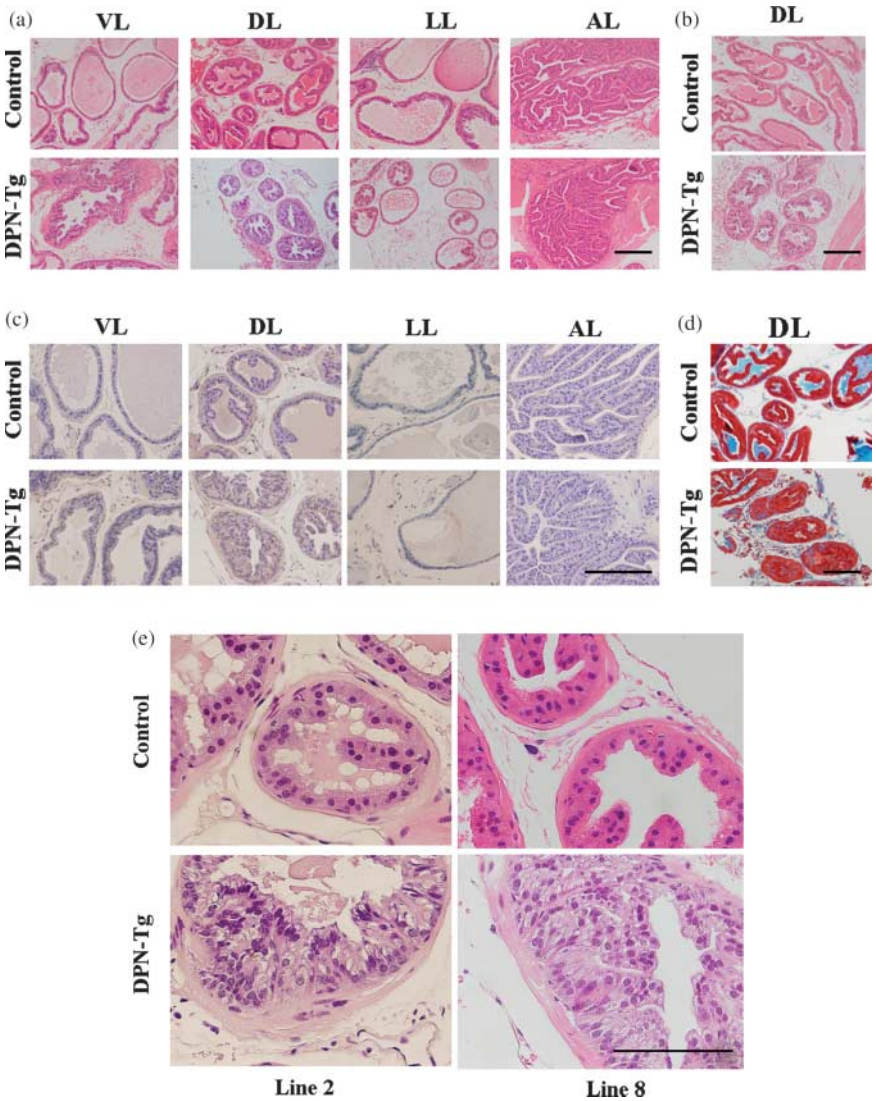

Figure 4 (a) Hematoxylin–eosin staining of the prostate of mouse dermatopontin transgenic mice line 8 at the age of 11 months; DPN-Tg, mouse dermatopontin transgenic; VL, ventral lobe; DL, dorsal lobe; LL, lateral lobe; AL, anterior lobe; bar=220 μm. (b) Hematoxylin–eosin staining of the prostatic dorsal lobe of mouse dermatopontin transgenic mice line 2, bar=200 μm. (c) Immunohistochemistry of dermatopontin in the prostate of mouse dermatopontin transgenic mice (line 8), bar=220 μm. (d) Masson-trichrome staining of the prostatic dorsal lobe of mouse dermatopontin transgenic mice (line 2), bar=160 μm. (e) Higher magnification of hematoxylin–eosin staining of the prostatic gland of the dorsal lobe of mouse dermatopontin transgenic mice at the age of 11 months; DPN-Tg, mouse dermatopontin transgenic; lines 2 and 8 indicate transgenic lines, bar=100 μm.

dermatopontin-transgenic prostate were much reduced by increasing gel concentration. Additionally, adsorption of anti-dermatopontin antibody with a peptide derived from mouse dermatopontin diminished transgenic dermatopontin signals. Thus, the usage of the anti-mouse dermatopontin polyclonal antibody in the immunohistochemistry of the mouse prostate seems appropriate. Possible dermatopontin receptor, detected with the f-DPN-AP, existed in the interstitium of the prostatic lobes. Again, this fusion protein might have simply detected other extracellular matrices combining with the mouse dermatopontin, but at least we can say that the prostatic epithelium does not possess targets of dermatopontin. The prostatic epithelium may not possess targets of dermatopontin or it may weakly express the targets below the sensitivity of the assay.

The dorsal lobe of dermatopontin transgenic mice expressing dermatopontin in the prostatic epithelium, but not that of control mice showed PIN at 11 months of age. Enhanced dermatopontin expression in the dorsal lobe might have

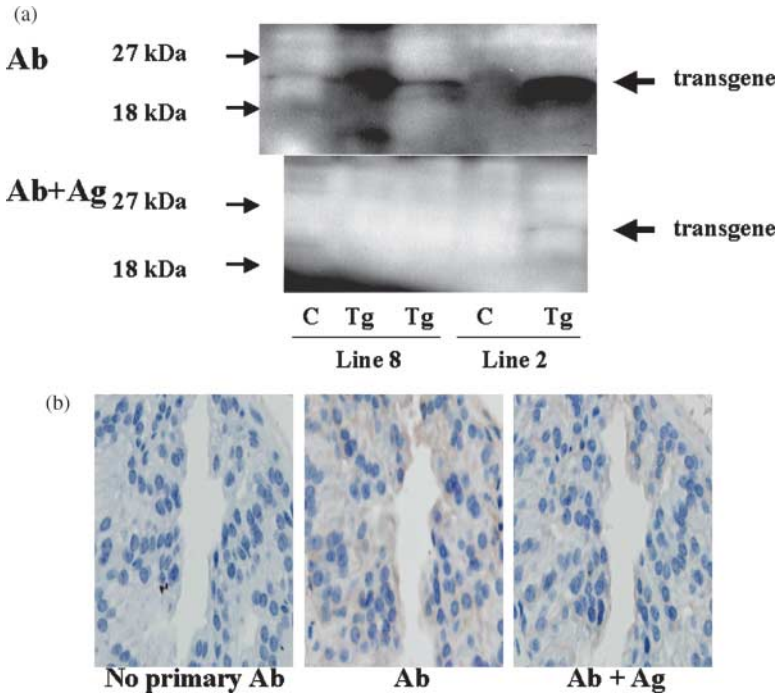

Figure 5 (a) Western blot analysis of dermatopontin protein, transgene: dermatopontin transgene; C, control; Tg, transgenic; Line, transgenic line. (b) Immunohistochemistry of dermatopontin in the epithelium of the prostatic dorsal lobe (line 8). No primary Ab, no primary antibody; Ab, dermatopontin polyclonal antibody; Ab+Ag, dermatopontin polyclonal antibody adsorbed with a dermatopontin peptide.

stimulated stromal cells, such as fibroblasts, endothelial cells and myocytes, via the targets of dermatopontin, then those stromal cells might have released growth factors and cytokines that cause prostatic epithelial proliferation leading to PIN. However, it is of note that the stroma surrounding the PIN is not significantly increased as compared to controls. There is also a possibility that enhanced epithelial expression of dermatopontin might have directly stimulated the targets of dermatopontin, expressed on the prostatic epithelium itself, but not detected with the fusion protein because of low assay sensitivity. Reasons why only the epithelium in the dorsal lobe of the dermatopontin transgenic mice showed PIN is basically unknown, while that in the ventral lobe also expressed dermatopontin. As the FGF-2 transgenic mice under the control of the short probasin promoter showed epithelial hyperplasia only in the dorsal lobe, but not in the ventral and lateral lobes (Konno-Takahashi *et al.* 2004), epithelium in the dorsal lobe may be the most sensitive to the proliferative stimulation of growth factors.

In conclusion, dermatopontin may be involved in the pathogenesis, growth, and metastasis of the prostate cancer. The mechanisms need to be further investigated in the future.

Acknowledgements

We are grateful to Mrs E Tanaka and Mrs A Hirose for assistance with cell culture and animal care respectively. This work was partially supported by the Ministry of Education, Science, Sports and Culture, Grant-in-Aid for Scientific Research (C), No. 14571488, 2002 to Takumi Takeuchi. The authors declare that there is no conflict of interest that would prejudice the impartiality of this scientific work.

References

Catherino WH, Leppert PC, Stenmark MH, Payson M, Potlog-Nahari C, Nieman LK & Segars JH 2004 Reduced dermatopontin expression is a molecular link between uterine leiomyomas and keloids. *Genes Chromosomes Cancer* **40** 204–217.

Diatchenko L, Lau CY, Campbell AP, Chenchik A, Moqadam F, Huang B, Lukyanov S, Lukyanov K, Gurskaya N, Sverdlov ED *et al.* 1996 Suppression subtractive hybridization: a method for generating differentially regulated or tissue-specific cDNA probes and libraries. *PNAS* **93** 6025–6030.

Festuccia C, Bologna M, Gravina GL, Guerra F, Angelucci A, Villanova I, Millimaggi D & Teti A 1999 Osteoblast conditioned media contain TGF-beta1 and modulate the migration of prostate tumor cells and their interactions with extracellular matrix components. *International Journal of Cancer* **81** 395–403.

Festuccia C, Angelucci A, Gravina GL, Villanova I, Teti A, Albini A & Bologna M 2000 Osteoblast-derived TGF-beta1 modulates matrix degrading protease expression and activity in prostate cancer cells. *International Journal of Cancer* **85** 407–415.

Forbes EG, Cronshaw AD, MacBeath JR & Hulmes DJ 1994 Tyrosine-rich acidic matrix protein (TRAMP) is a tyrosine-sulphated and widely distributed protein of the extracellular matrix. *FEBS Letters* **351** 433–436.

Hepburn PJ, Griffiths K & Harper ME 1997 Angiogenic factors expressed by human prostatic cell lines: effect on endothelial cell growth in vitro. *Prostate* **33** 123–132.

Kim IY, Ahn HJ, Zelner DJ, Shaw JW, Sensibar JA, Kim JH, Kato M & Lee C 1996 Genetic change in transforming growth factor beta (TGF-beta) receptor type I gene correlates with insensitivity to TGF-beta 1 in human prostate cancer cells. *Cancer Research* **56** 44–48.

Konno-Takahashi N, Takeuchi T, Shimizu T, Nishimatsu H, Fukuhara H, Kamijo T, Moriyama N, Tejima S & Kitamura T 2003 Engineered IGF-I expression induces glandular enlargement in the murine prostate. *Journal of Endocrinology* **177** 389–398.

Konno-Takahashi N, Takeuchi T, Nishimatsu H, Kamijo T, Tomita K, Schalken JA, Tejima S & Kitamura T 2004 Engineered FGF-2 expression induces glandular epithelial hyperplasia in the murine prostatic dorsal lobe. *European Urology* **46** 126–132.

Kuroda K, Okamoto O & Shinkai H 1999 Dermatopontin expression is decreased in hypertrophic scar and systemic sclerosis skin fibroblasts and is regulated by transforming growth factor-beta1, interleukin-4, and matrix collagen. *Journal of Investigative Dermatology* **112** 706–710.

Nakamoto T, Chang CS, Li AK & Chodak GW 1992 Basic fibroblast growth factor in human prostate cancer cells. *Cancer Research* **52** 571–577.

Neame PJ, Choi HU & Rosenberg LC 1989 The isolation and primary structure of a 22 kDa extracellular matrix protein from bovine skin. *Journal of Biological Chemistry* **264** 5474–5479.

Niwa H, Yamamura K & Miyazaki J 1991 Efficient selection for high-expression transfectant with a novel eukaryotic vector. *Gene* **108** 193–199.

Okamoto O, Suzuki Y, Kimura S & Shinkai H 1996 Extracellular matrix 22 kDa protein interacts with decorin core protein and is expressed in cutaneous fibrosis. *Journal of Biochemistry (Tokyo)* **119** 106–114.

Okamoto O, Fujiwara S, Abe M & Sato Y 1999 Dermatopontin interacts with transforming growth factor beta and enhances its biological activity. *Biochemical Journal* **337** 537–541.

Rennie PS, Bruchovsky N, Leco KJ, Sheppard PC, McQueen SA, Cheng H, Snoek R, Hamel A, Bock ME, MacDonald BS *et al.* 1993 Characterization of two cis-acting DNA elements involved in the androgen regulation of the probasin gene. *Molecular Endocrinology* **7** 23–36.

Rosini P, Bonaccorsi L, Baldi E, Chiasserini C, Forti G, De Chiara G, Lucibello M, Mongiat M, Iozzo RV, Garaci E *et al.* 2002 Androgen receptor expression induces FGF2, FGF-binding protein production, and FGF2 release in prostate carcinoma cells: role of FGF2 in growth, survival, and androgen receptor down-modulation. *Prostate* **53** 310–321.

Shappell SB, Thomas GV, Roberts RL, Herbert R, Ittmann MM, Rubin MA, Humphrey PA, Sundberg JP, Rozengurt N, Barrios R *et al.* 2004 Prostate pathology of genetically engineered mice: definitions and classification. The consensus report from the Bar Harbor Meeting of the Mouse Models of Human Cancer Consortium Prostate Pathology Committee. *Cancer Research* **64** 2270–2305.

Superti-Furga A, Rocchi M, Schafer BW & Gitzelmann R 1993 Complementary DNA sequence and chromosomal mapping of a human proteoglycan-binding cell-adhesion protein (dermatopontin). *Genomics* **17** 463–467.

Takeda U, Utani A, Wu J, Adachi E, Koseki H, Taniguchi M, Matsumoto T, Ohashi T, Sato M & Shinkai H 2002 Targeted disruption of dermatopontin causes abnormal collagen fibrillogenesis. *Journal of Investigative Dermatology* **119** 678–683.

Takemoto S, Murakami T, Kusachi S, Iwabu A, Hirohata S, Nakamura K, Sezaki S, Havashi J, Suezawa C, Ninomiya Y *et al.* 2002 Increased expression of dermatopontin mRNA in the infarct zone of experimentally induced myocardial infarction in rats: comparison with decorin and type I collagen mRNAs. *Basic Research in Cardiology* **97** 461–468.

Takeuchi T, Sasaki Y, Ueki T, Kaziwara T, Moriyama N, Kawabe K & Kakizoe T 1996 Modulation of growth and apoptosis response in PC-3 and LNCAP prostate-cancer cell lines by Fas. *International Journal of Cancer* **67** 709–714.

Takeuchi T, Ueki T, Nishimatsu H, Kajiwara T, Ishida T, Jishage K, Ueda O, Suzuki H, Li B, Moriyama N *et al.* 1999 Accelerated rejection of Fas-ligand expressing heart grafts. *Journal of Immunology* **162** 518–522.

Takeuchi T, Nishimatsu H, Ueki T, Kajiwara T, Fukuhara H, Ishida T, Moriyama N & Kitamura T 2000 Differentially expressed mRNAs in androgen-independent but not androgen-dependent Shionogi carcinoma. *Urological Research* **28** 82–85.

Tsibris JC, Segars J, Coppola D, Mane S, Wilbanks GD, O'Brien WF & Spellacy WN 2002 Insights from gene arrays on the development and growth regulation of uterine leiomyomata. *Fertility and Sterility* **78** 114–121.

Tzen CY & Huang YW 2004 Cloning of murine early quiescence-1 gene: the murine counterpart of dermatopontin gene can induce and be induced by cell quiescence. *Experimental Cell Research* **294** 30–38.

Wilding G, Zugmeier G, Knabbe C, Flanders K & Gelmann E 1989 Differential effects of transforming growth factor beta on human prostate cancer cells in vitro. *Molecular and Cellular Endocrinololy* **62** 79–87.

Received in final form 27 April 2006
Accepted 27 April 2006
Made available online as an Accepted Preprint
10 May 2006